

University of Groningen

## Nature-inspired microfluidic propulsion using magnetic actuation

Khaderi, S. N.; Baltussen, M. G. H. M.; Anderson, P. D.; Ioan, D.; den Toonder, J.M.J.; Onck, P. R.

*Published in:*  
Physical Review E

*DOI:*  
[10.1103/PhysRevE.79.046304](https://doi.org/10.1103/PhysRevE.79.046304)

**IMPORTANT NOTE: You are advised to consult the publisher's version (publisher's PDF) if you wish to cite from it. Please check the document version below.**

*Document Version*  
Publisher's PDF, also known as Version of record

*Publication date:*  
2009

[Link to publication in University of Groningen/UMCG research database](#)

*Citation for published version (APA):*

Khaderi, S. N., Baltussen, M. G. H. M., Anderson, P. D., Ioan, D., den Toonder, J. M. J., & Onck, P. R. (2009). Nature-inspired microfluidic propulsion using magnetic actuation. *Physical Review E*, 79(4), 046304-1-046304-4. [046304]. <https://doi.org/10.1103/PhysRevE.79.046304>

### Copyright

Other than for strictly personal use, it is not permitted to download or to forward/distribute the text or part of it without the consent of the author(s) and/or copyright holder(s), unless the work is under an open content license (like Creative Commons).

### Take-down policy

If you believe that this document breaches copyright please contact us providing details, and we will remove access to the work immediately and investigate your claim.

*Downloaded from the University of Groningen/UMCG research database (Pure): <http://www.rug.nl/research/portal>. For technical reasons the number of authors shown on this cover page is limited to 10 maximum.*

**Supporting information for the paper "Nature-inspired  
microfluidic propulsion using magnetic actuation"**

S. N. Khaderi, M. G. H. M. Baltussen, P. D. Anderson,  
D. Ioan, J. M. J. den Toonder, and P. R. Onck

## I. EQUATIONS OF MOTION

The artificial cilia are modelled as a discrete assemblage of Euler-Bernoulli beam elements. The beam element has two nodes at the ends and has three degree of freedom (DOF) at each node:  $u$  the axial displacement,  $v$  the transverse displacement and  $\phi = \partial v / \partial x$  the rotation, where  $x$  is the axial coordinate along the beam. The axial displacement along the beam (or film) is interpolated linearly and the transverse displacement is interpolated cubically,

$$u = \mathbf{N}_u \mathbf{p}, \quad v = \mathbf{N}_v \mathbf{p}, \quad (1)$$

where  $\mathbf{N}_u$  and  $\mathbf{N}_v$  being the standard interpolation matrices [1] and  $\mathbf{p} = \{u_1 \ v_1 \ \phi_1 l_0 \ u_2 \ v_2 \ \phi_2 l_0\}^T$ , where the subscripts 1 and 2 refer to the node numbers and  $l_0$  is some reference length. The nonlinear axial strain  $\epsilon$  in the beam is

$$\epsilon = \frac{\partial u}{\partial x} + \frac{1}{2} \left( \frac{\partial v}{\partial x} \right)^2 - y \frac{\partial^2 v}{\partial x^2} \equiv \bar{\epsilon} - y\chi.$$

The principle of virtual work is used as a condition to establish equilibrium [2]: When a consistent virtual displacement field is applied on a body, the body will be in equilibrium when the virtual work done by the internal forces equals the virtual work done by the external force,

$$\delta W_{\text{int}}^{t+\Delta t} = \delta W_{\text{ext}}^{t+\Delta t},$$

with

$$\delta W_{\text{int}}^{t+\Delta t} = \int_{V_0} (\sigma \delta \epsilon + \rho (\ddot{u} \delta u + \ddot{v} \delta v)) dV,$$

where  $\delta(\cdot)$  represents the variation of a quantity,  $\sigma$  is the axial stress,  $\rho$  is the density of the film and a  $(\ddot{\cdot})$  implies a second derivative w.r.t. time. By substituting the strains and defining  $\int \sigma dA = P$  and  $-\int \sigma y dA = M$  ( $A = bh$  is the area of the cross section,  $h$  is the thickness and  $b$  is the out-of-plane width of the film), the internal virtual work at time  $t + \Delta t$  can be written as the sum of an elastic and an inertial part

$$\delta W_{\text{int}}^{t+\Delta t} = \int_{x_0} (P^{t+\Delta t} \delta \bar{\epsilon}^{t+\Delta t} + M^{t+\Delta t} \delta \chi + \rho A (\ddot{u}^{t+\Delta t} \delta u + \ddot{v}^{t+\Delta t} \delta v)) dx.$$

We now expand the elastic part of the internal work linearly in time by substituting ( $Q^{t+\Delta t} = Q^t + \Delta Q$ ) for the field parameters in Eqn. 2 which gives

$$\delta W_{\text{int}}^{t+\Delta t} = \int_{x_0} [ (P^t \delta \bar{\epsilon}^t + M^t \delta \chi) + (\Delta P \delta \bar{\epsilon}^t + \Delta M \delta \chi) + P^t \Delta \delta \bar{\epsilon} + \rho A (\ddot{u}^{t+\Delta t} \delta u + \ddot{v}^{t+\Delta t} \delta v) ] dx,$$

in which terms of order higher than one are neglected. The following notations are introduced for convenience:  $\partial u / \partial x = \mathbf{B}_u \mathbf{p}$ ,  $\partial v / \partial x = \mathbf{B}_v \mathbf{p}$ ,  $\partial^2 u / \partial x^2 = \mathbf{C}_v \mathbf{p}$ . The constitutive relations are  $\Delta P = EA \Delta \bar{\epsilon}$ ,  $\Delta M = EI \Delta \chi$ , with  $E = \bar{E} / (1 - \nu^2)$  being the effective elastic modulus,  $\nu$  being the Poisson's ratio and  $I$  being the second moment of area defined as  $I = bh^3 / 12$ . By choosing the domain of integration to be the current configuration (i.e. using an updated Lagrangian framework), the total displacements are zero,  $\mathbf{p} = 0$  and we get

$$\delta W_{\text{int}}^{t+\Delta t} = \delta \mathbf{p}^T \mathbf{f}_{\text{int}}^t + \delta \mathbf{p}^T \mathbf{K} \Delta \mathbf{p} + \delta \mathbf{p}^T \mathbf{M} \ddot{\mathbf{p}}^{t+\Delta t}, \quad (2)$$

where

$$\mathbf{f}_{\text{int}}^t = \int [ P^t \mathbf{B}_u^T + M^t \mathbf{C}_v^T ] dx$$

is the nodal internal force vector,

$$\mathbf{K} = \int E A \mathbf{B}_u^T \mathbf{B}_u dx + \int E I \mathbf{C}_v^T \mathbf{C}_v dx + \int P^t \mathbf{B}_v^T \mathbf{B}_v dx$$

is the stiffness matrix, the first two terms of which represent the material stiffness and the third term represents the geometric stiffness, and

$$\mathbf{M} = \int \rho A (\mathbf{N}_u^T \mathbf{N}_u + \mathbf{N}_v^T \mathbf{N}_v) dx$$

is the mass matrix. The corresponding external virtual work is

$$\begin{aligned} \delta W_{\text{ext}}^{t+\Delta t} &= \int \left( f_x^{t+\Delta t} \delta u + f_y^{t+\Delta t} \delta v + N_z^{t+\Delta t} \frac{\partial \delta v}{\partial x} \right) A dx + \int (t_x^{t+\Delta t} \delta u + t_y^{t+\Delta t} \delta v) b dx \\ &= \delta \mathbf{p}^T \int [ (f_x^{t+\Delta t} \mathbf{N}_u^T + f_y^{t+\Delta t} \mathbf{N}_v^T + N_z^{t+\Delta t} \mathbf{B}_v^T) A + b (t_x^{t+\Delta t} \mathbf{N}_u^T + t_y^{t+\Delta t} \mathbf{N}_v^T) ] dx \\ &= \delta \mathbf{p}^T \mathbf{f}_{\text{ext}}^{t+\Delta t}, \end{aligned} \quad (3)$$

where  $f_x$  and  $f_y$  are the body forces in axial and transverse directions (for example, magnetic body forces),  $N_z$  is the body couple in the out-of-plane direction (for example, magnetic body couple) and  $t_x$  and  $t_y$  are the surface tractions (for example, fluid drag). By equating the internal and external virtual work and noting that the resulting equation holds for arbitrary  $\delta \mathbf{p}$  we get

$$\mathbf{K} \Delta \mathbf{p} + \mathbf{M} \ddot{\mathbf{p}}^{t+\Delta t} = \mathbf{f}_{\text{ext}}^{t+\Delta t} - \mathbf{f}_{\text{int}}^t. \quad (4)$$

The motion of the film with time is obtained by solving Eqn. 4 using Newmark's algorithm with appropriate initial and boundary conditions. In the next two sections we will discuss how the fluid forces (section II) and the magnetic forces (section III) in Eqn. 3 are obtained.

## II. FLUID FORCES

The drag forces of the fluid on the film can be accounted for in an uncoupled manner using drag forces or by coupled solid-fluid interaction. In the former approach the tractions in Eqn. 3 are assumed to be proportional to the velocity in the low Reynolds number regime,

$$t_x = -C_x v_x, \quad t_y = -C_y v_y, \quad (5)$$

where  $t_x$  and  $t_y$  is the traction exerted by the fluid in axial and transverse direction to the film, respectively,  $C_x$  and  $C_y$  are the axial and transverse drag coefficients, respectively and  $v_x$  and  $v_y$  are the respective axial and transverse velocities. This assumption is in the spirit of the resistive force theory [3]. For the finite element discretization, the drag force is assumed to vary linearly along the film. Analytical expressions for the drag coefficients are available only for simple rigid geometries, but as the film is modelled as a deforming slender object such analytical expressions are not available. Hence, we calibrate these drag coefficients with reference to the coupled solid-fluid model.

The Lagrangian solid dynamics model used to study the magneto-mechanical behavior of the films (Section I) is coupled to an Eulerian fluid dynamics code based on the method detailed in [4]. The explicit coupling between the two domains is established through Lagrange multipliers. Input to the fluid dynamics model are the positions and velocities of the film at all times which result in a full velocity field in the fluid. Fluid inertia is neglected, so

the fluid model effectively solves the Stokes equations. We calculate the drag forces on the film as tractions via the stress tensor in the fluid. The traction distribution is subsequently imposed as surface tractions in the solid dynamics model through Eqn. 3.

The calibration is done as follows. First, a simulation using the coupled solid-fluid code is performed and the trajectory of the free end is noted. Then, simulations are performed using the solid dynamic model with velocity-proportional drag forces using some assumed drag coefficients. The trajectory thus obtained is matched with the trajectory obtained from the coupled solid-fluid code by varying the drag coefficients. The calibrated drag coefficients are  $C_x = 8.75 \text{ Ns/m}^3$  and  $C_y = 105 \text{ Ns/m}^3$  for the PM film and  $C_x = 80 \text{ Ns/m}^3$  and  $C_y = 160 \text{ Ns/m}^3$  for the SPM film. A comparison between the coupled solid-fluid model and the uncoupled solid-drag model is shown in Figs. 1(a) and 1(b), showing good agreement, especially for the SPM configuration. The discrepancy between the two trajectories comes from the fact that the resistive force theory does not account for the interaction of the film with the substrate and with itself.

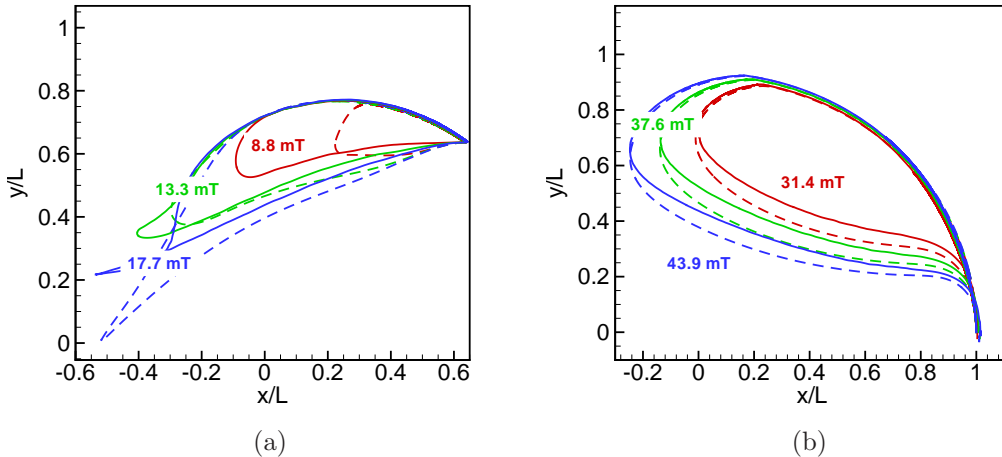


FIG. 1: The trajectory of the free end for the PM configuration (a) and the SPM configuration (b) for three different values of the applied magnetic field. The solid lines are for the coupled solid-fluid simulations and the dashed lines for the uncoupled solid-drag calculations.

### III. MAGNETOSTATICS

The magnetic forces come in through the body forces and couples in Eqn. 3. To find the resulting magnetic forces, the magnetic field has to be calculated in the deformed configu-

ration of the film at every time increment as a function of the externally applied magnetic field. Maxwell's equations for the magnetostatic problem with no currents are

$$\nabla \cdot \mathbf{B} = 0 \quad \nabla \times \mathbf{H} = 0, \quad (6)$$

with the constitutive relation  $\mathbf{B} = \mu_0(\mathbf{M} + \mathbf{H})$ , where  $\mathbf{B}$  is the magnetic flux density (or magnetic induction),  $\mathbf{H}$  is the magnetic field,  $\mathbf{M}$  is the magnetization which includes the remnant magnetization, and  $\mu_0$  is the permeability of vacuum. By taking into consideration the effect of discontinuity in the medium, the general solution of the Maxwell's equations (Eqn. 6) is given by the Green's function [5],

$$\mathbf{H}(\mathbf{x}) = -\frac{1}{4\pi} \nabla \oint \frac{\mathbf{n}' \cdot \mathbf{M}(\mathbf{x}')}{|\mathbf{x} - \mathbf{x}'|} dS' + \frac{1}{4\pi} \nabla \int \frac{\nabla' \cdot \mathbf{M}(\mathbf{x}')}{|\mathbf{x} - \mathbf{x}'|} dV'. \quad (7)$$

where  $\mathbf{n}'$  is the outward normal to the surface of  $V$ . By assuming that the magnetization is uniform inside the volume, so  $\nabla' \cdot \mathbf{M} = 0$ , the volume integral vanishes, and the field is only due to the jump of magnetization across the surface, as reflected by the surface integral in Eqn. 7.

We now discretize the film into a chain of rectangular segments. The magnetization  $\mathbf{M}$  is uniform inside and zero outside the segment. The magnetic field due to the four surfaces of the  $i^{\text{th}}$  segment can now be calculated at any  $j^{\text{th}}$  segment by evaluating the surface integral in Eqn. 7, resulting in  $\mathbf{H}_j = \mathbf{G}_{ji}(\mathbf{x}_j - \mathbf{x}_i) \mathbf{M}_i$  (the Einstein summation convention does not apply here), where  $\mathbf{H}$  is the field in the  $j^{\text{th}}$  segment,  $\mathbf{G}_{ji}(\mathbf{x}_j - \mathbf{x}_i)$  is a function of the distance between the segments  $i$  and  $j$  and the geometry of segment  $i$  and  $\mathbf{M}_i$  is the magnetization of the  $i^{\text{th}}$  segment.

The field at any element  $j$  because of the magnetization of all the segments throughout the film is

$$\mathbf{H}_j = \mathbf{H}_0 + \sum_{i=1}^N \mathbf{G}_{ji} \mathbf{M}_i, \quad (8)$$

where  $\mathbf{H}_0$  is the externally applied magnetic field and  $N$  is the total number of segments. For the situation of a permanently magnetized film with magnetization  $\mathbf{M}_i$ ,  $i = 1, \dots, N$ , Eqn. 8 gives the magnetic field in all the segments.

However, in case of a super-paramagnetic film, the magnetization  $\mathbf{M}_j$  is not known a-priori, but depends on the local magnetic field through

$$\mathbf{M}_j = \boldsymbol{\chi} \mathbf{H}_j = \boldsymbol{\chi} \mathbf{H}_0 + \sum_{i=1}^N \boldsymbol{\chi} \mathbf{G}_{ij} \mathbf{M}_i, \quad (9)$$

with  $\boldsymbol{\chi}$  is the susceptibility tensor (which can be anisotropic). There are  $N$  similar pairs of equations. In total these are  $2 \times N$  equations for the  $2 \times N$  unknown magnetizations, which need to be solved. Once the magnetization is known the field can be found from Eqn. 8. Then the magnetic flux density can be found by using the constitutive equation. The magnetic couple per unit volume is given by  $\mathbf{N} = \mathbf{M} \times \mathbf{B}$ . Since a uniform magnetic field is applied, the magnetic body forces due to field gradients are neglected in the present study.

- 
- [1] R. D. Cook, D. Malkus, M. Plesha, D. S. Malkus, and M. E. Plesha, *Concepts and Applications of Finite Element Analysis* (John Wiley and sons, 2001).
  - [2] L. E. Malvern, *Introduction to the Mechanics of a Continuous Medium* (Prentice-Hall, 1977).
  - [3] R. E. Johnson and C. J. Brokaw, *Biophys. J.* **25**, 113 (1979).
  - [4] F. P. T. Baaijens, *International Journal for Numerical Methods in Fluids* **35**, 743 (2001).
  - [5] J. D. Jackson, *Classical Electrodynamics* (John Wiley and sons, 1974).